Vietnam Journal of Mechanics, VAST, Vol. 42, No. 2 (2020), pp. 189 – 205
DOI: https://doi.org/10.15625/0866-7136/14817

FREE VIBRATION OF A 2D-FGSW BEAM BASED ON A SHEAR DEFORMATION THEORY

Vu Thi An Ninh[1,*], **Le Thi Ngoc Anh**[2,3], **Nguyen Dinh Kien**[3,4]
[1]*University of Transport and Communications, Hanoi, Vietnam*
[2]*Institute of Applied Mechanics and Informatics, Ho Chi Minh city, Vietnam*
[3]*Graduate University of Science and Technology, VAST, Hanoi, Vietnam*
[4]*Institute of Mechanics, VAST, Hanoi, Vietnam*
[*]E-mail: vuthianninh@gmail.com

Received: 10 February 2020 / Published online: 19 May 2020

Abstract. A two-dimensional functionally graded sandwich (2D-FGSW) beam model formed from three constituent materials is proposed and its free vibration is studied for the first time. The beam consists of three layers, a homogeneous core and two functionally graded skin layers with material properties varying in both the length and thickness directions by power gradation laws. Based on a third-order shear deformation theory, a beam element using the transverse shear rotation as an independent variable is formulated and employed in the study. The obtained numerical result reveals that the variation of the material properties in the length direction plays an important role on the natural frequencies and vibration modes of the beam. The effects of the material distribution and layer thickness ratio on the vibration characteristics are investigated in detail. The influence of the aspect ratio on the frequencies is also examined and discussed.

Keywords: 2D-FGSW beam, third-order shear deformation theory, transverse shear rotation, free vibration, finite element method.

1. INTRODUCTION

With the development of advanced manufacturing methods [1], functionally graded materials (FGMs), a new type of composite material initiated by Japanese researchers in mid-1980 [2], can now be incorporated into sandwich construction to improve performance of the structures. Functionally graded sandwich (FGSW) structures can be designed to have a smooth variation of properties, which helps to avoid the interface separation problem as often seen in the conventional sandwich structures. Investigations on mechanical behaviour of FGSW structures have been intensively reported in recent years, contributions that are most relevant to present work are briefly discussed below.

Chakraborty et al. [3] derived a beam element for thermoelastic analysis of FGM beams and FGSW beams. The element employing the solution of static equilibrium equations of a Timoshenko beam segment to interpolate the displacement field is free of the shear locking. Different beam theories were employed by Apetre et al. [4] to study static bending of the sandwich beams with an FGM core. The modified differential quadrature method was used by Pradhan and Murmu [5] to investigate thermomechanical vibration of FGM and FGSW beams supported by a foundations. Rahmani et al. [6] considered free vibration of sandwich beams with a syntactic core using a higher-order sandwich panel theory. The element free Galerkin and mesh-free radial point interpolation methods were employed by Amirani et al. [7] to perform vibration analysis of sandwich beams with an FGM core. Based on a sinusoidal shear deformation beam theory, Zenkour et al. [8] investigated the bending response of an FGM viscoelastic sandwich beam resting on a Pasternak foundation. The refined shear deformation theories in which the transverse displacement is split into bending and shear parts were employed by Vo et al. [9, 10] to study free vibration and buckling of FGSW beams. Bennai et al. [11] considered vibration and buckling of FGSW beams using a refined hyperbolic shear and normal deformation beam theory. The frequencies of FGSW beams resting on an elastic foundation were evaluated by Su et al. [12] using a modified Fourier method. Şimşek and Al-shujairi [13] investigated bending and vibration of FGSW beams using a semi-analytical method. Finite element method was used to study free vibration of functionally graded carbon nanotubes reinforced laminated beams [14].

The sandwich beams in the above discussed references have material properties varying in the thickness direction only. There are practical circumstances, in which the unidirectional FGMs may not be so appropriate to resist multi-directional variations of thermal and mechanical loadings. For example, the temperature on the outer surface of the new aerospace craft in sustained flight can range from 1033K along the top of the fuselage to 2066K at the nose and from outer surface temperature to room temperature inside the plane [15]. Development of FGM and FGSW beams with effective material properties varying in two or more directions to withstand severe general loadings is of great importance in practice [15, 16]. Several models for bi-dimensional FGM beams and their mechanical behaviour have been considered recently. In this line of works, Şimşek [17] considered the material properties vary in both the length and thickness directions, by an exponential function in vibration study of a Timoshenko beam. Polynomials were assumed for the displacement field in computing natural frequencies and dynamic response of the beam. Wang et al. [18] presented an analytical method for free vibration analysis of a 2D-FGM beam. The material properties are also assumed to vary exponentially in the beam thickness and length. Bending of a two-dimensional FGM sandwich (2D-FGSW) beam was investigated by Karamanli [19] using a quasi-3D shear deformation theory and a symmetric smoothed particle hydrodynamics method. Nguyen et al. [20] proposed a 2D-FGM beam model formed from four different constituent materials with volume fractions to vary by power-law functions in both the thickness and longitudinal directions. Timoshenko beam theory was adopted by the authors in evaluating dynamic response of the beam to a moving load. The beam model has been adopted by Tran and Nguyen [21] in examining the thermal effect of free vibration of the beam.

In this paper, a two-dimensional functionally graded sandwich (2D-FGSW) beam model formed from three constituent materials is proposed and its free vibration analysis is carried out for the first time. The beam consists of three layers, a homogeneous core and two skin layers of 2D-FGM. The material properties of the skin layers are considered to vary in both the thickness and longitudinal directions by power gradation laws. Based on a third-order shear deformation theory, a beam element using the transverse rotation as an independent variable is formulated and employed to compute vibration characteristics. Numerical investigation is carried out to show the accuracy of the derived element and to illustrate the effects of the material distribution and layer thickness ratio on vibration frequencies and vibration modes of the beam.

2. 2D-FGSW BEAM MODEL

A 2D-FGSW beam model formed from three distinct materials, material 1 (M1), material 2 (M2) and material 3 (M3), as depicted in Fig. 1 is proposed herein. The beam with rectangular cross section consists of three layers, a fully core of M1 and two 2D-FGM skin layers of M1, M2 and M3. The Cartesian coordinates (x, z) in the figure is chosen such that the x-axis is on the mid-plane and the z-axis directs upward. Denoting z_0, z_3, z_1 and z_2 are, respectively, the vertical coordinates of the bottom and top surfaces, and the interfaces of the layers. The volume fraction of M1, M2 and M3 are assumed to vary in the x- and z-directions according to

$$\text{for } z \in [z_0, z_1] \qquad \begin{cases} V_1 &= \left(\dfrac{z-z_0}{z_1-z_0}\right)^{n_z} \\ V_2 &= \left[1-\left(\dfrac{z-z_0}{z_1-z_0}\right)^{n_z}\right]\left[1-\left(\dfrac{x}{L}\right)^{n_x}\right] \\ V_3 &= \left[1-\left(\dfrac{z-z_0}{z_1-z_0}\right)^{n_z}\right]\left(\dfrac{x}{L}\right)^{n_x} \end{cases}$$

$$\text{for } z \in [z_1, z_2] \qquad V_1 = 1, V_2 = V_3 = 0 \tag{1}$$

$$\text{for } z \in [z_2, z_3] \qquad \begin{cases} V_1 &= \left(\dfrac{z-z_3}{z_2-z_3}\right)^{n_z} \\ V_2 &= \left[1-\left(\dfrac{z-z_3}{z_2-z_3}\right)^{n_z}\right]\left[1-\left(\dfrac{x}{L}\right)^{n_x}\right] \\ V_3 &= \left[1-\left(\dfrac{z-z_3}{z_2-z_3}\right)^{n_z}\right]\left(\dfrac{x}{L}\right)^{n_x} \end{cases}$$

where V_1, V_2 and V_3 are, respectively, the volume fraction of the M1, M2 and M3; n_x and n_z are the material grading indexes, defining the variation of the constituents in the x and z directions, respectively. As seen from Eq. (1), the top and bottom corners at the left end of the beam are pure M2, while the corresponding corners at the right end are pure M3. The model defines a softcore sandwich beam if M1 is a metal, and it is a hardcore one if M1 is a ceramic. Fig. 2 shows the variation of V_1, V_2 and V_3 in the thickness and length directions for $n_x = n_z = 0.5$, and $z_1 = -h/10$, $z_2 = h/10$.

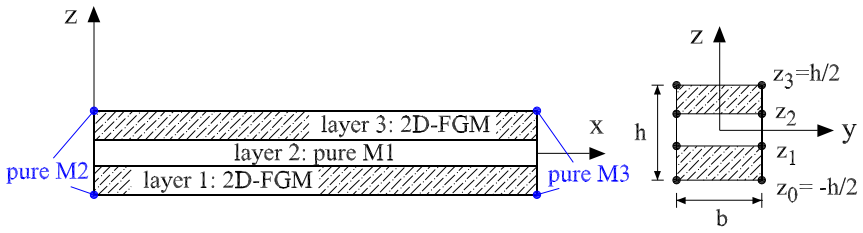

Fig. 1. A 2D-FGSW beam model formed from three materials

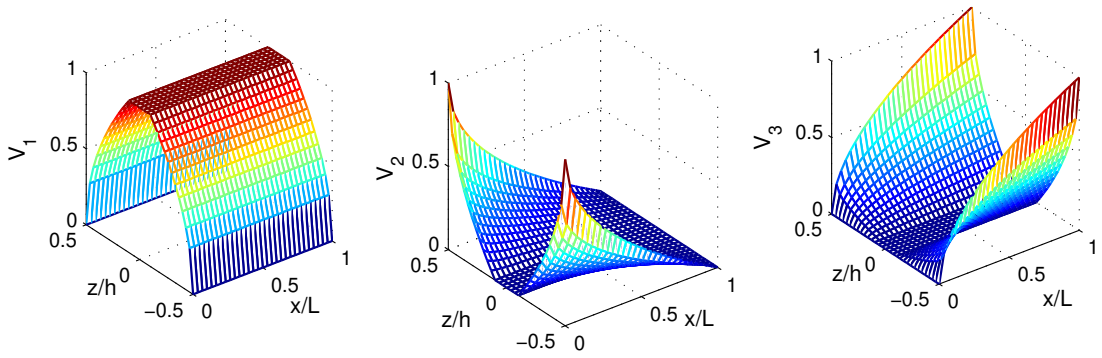

Fig. 2. Variation of V_1, V_2 and V_3 of 2D-FGSW beam for $n_x = n_z = 0.5$ and $z_1 = -h/10, z_2 = h/10$

The effective material properties $\mathcal{P}_f^{(k)}$ of the kth layer $(k = 1,\ldots,3)$ evaluated by Voigt's model are of the form

$$\mathcal{P}_f^{(k)} = \mathcal{P}_1 V_1 + \mathcal{P}_2 V_2 + \mathcal{P}_3 V_3, \tag{2}$$

where $\mathcal{P}_f^{(k)}$ represents the effective material properties such as mass density $\rho_f^{(k)}$, elastic modulus $E_f^{(k)}$ and shear modulus $G_f^{(k)}$; $\mathcal{P}_1$, $\mathcal{P}_2$, and $\mathcal{P}_3$ are, respectively, the properties of the M1, M2 and M3. Substituting Eq. (1) into Eq. (2) one gets

$$\mathcal{P}_f^{(k)}(x,z) = \begin{cases} [\mathcal{P}_1 - \mathcal{P}_{23}(x)]\left(\dfrac{z-z_0}{z_1-z_0}\right)^{n_z} + \mathcal{P}_{23}(x) & \text{for} \quad z \in [z_0, z_1] \\ \mathcal{P}_1 & \text{for} \quad z \in [z_1, z_2] \\ [\mathcal{P}_1 - \mathcal{P}_{23}(x)]\left(\dfrac{z-z_3}{z_2-z_3}\right)^{n_z} + \mathcal{P}_{23}(x) & \text{for} \quad z \in [z_0, z_1] \end{cases} \tag{3}$$

with $\mathcal{P}_{23}(x) = \mathcal{P}_2 - (\mathcal{P}_2 - \mathcal{P}_3)\left(\dfrac{x}{L}\right)^{n_x}$. One can easily verity that if $n_x = 0$ or M2 is identical to M3, Eq. (3) returns to the expression for the effective material properties of unidirectional FGSW beam in [9]. Furthermore, if $n_z = 0$, Eq. (3) reduces to property of a homogeneous beam of M1.

3. MATHEMATICAL MODEL

The third-order shear deformation theory recently proposed by Shi [22] is adopted herein. According to the theory, the displacements of a point in x- and z-directions, $u_1(x,z,t)$ and $u_3(x,z,t)$, respectively, are given by

$$\begin{aligned} u_1(x,z,t) &= u(x,t) + \frac{z}{4}(5\theta + w_{,x}) - \frac{5z^3}{3h^2}(\theta + w_{,x}), \\ u_3(x,z,t) &= w(x,t), \end{aligned} \tag{4}$$

where t is the time variable; z is the distance from the point to the x-axis; $u(x,t)$ and $w(x,t)$ are, respectively, the axial and transverse displacements of the point on the x-axis; $\theta(x,t)$ is the cross-sectional rotation. A subscript comma in Eq. (4) and hereafter is used to denote the derivative with respect to the variable which follows.

Following the work in [21], the transverse shear rotation, $\gamma_0 = \theta + w_{,x}$, is employed herewith as an independent variable. In this regard, we can rewrite the displacements in (4) in the form

$$\begin{aligned} u_1(x,z,t) =& u(x,t) + \frac{z}{4}(5\gamma_0 - 4w_{,x}) - \frac{5z^3}{3h^2}\gamma_0, \\ u_3(x,z,t) =& w(x,t). \end{aligned} \tag{5}$$

The axial strain (ε_{xx}) and shear strain (γ_{xz}) resulted from Eq. (5) are of the forms

$$\varepsilon_{xx} = u_{,x} + \frac{z}{4}(5\gamma_{0,x} - 4w_{,xx}) - \frac{5z^3}{3h^2}\gamma_{0,x}\,, \quad \gamma_{xz} = \frac{5}{4h^2}(h^2 - 4z^2)\gamma_0. \tag{6}$$

The constitutive equation for the beam is of the form

$$\begin{Bmatrix} \sigma_{xx} \\ \tau_{xz} \end{Bmatrix} = \begin{bmatrix} E_f^{(k)}(x,z) & 0 \\ 0 & G_f^{(k)}(x,z) \end{bmatrix} \begin{Bmatrix} \varepsilon_{xx} \\ \gamma_{xz} \end{Bmatrix} \tag{7}$$

where $E_f^{(k)}(x,z)$ and $G_f^{(k)}(x,z)$, are, respectively, the elastic and shear moduli, defined by Eq. (3); σ_{xx} and τ_{xz} are the axial stress and shear stress, respectively.

The strain energy U of the beam resulted from Eqs. (6) and (7) is of the form

$$\begin{aligned} U &= \frac{1}{2}\int_0^L \int (\sigma_{xx}\varepsilon_{xx} + \tau_{xz}\gamma_{xz})\,\mathrm{d}A\mathrm{d}x \\ &= \frac{1}{2}\int_0^L \Big[A_{11}u_{,x}^2 + 2A_{12}u_{,x}\Big(\frac{5}{4}\gamma_{0,x} - w_{,xx}\Big)^2 - \frac{10}{3h^2}\,A_{34}\,u_{,x}\gamma_{0,x} \\ &\quad - \frac{10}{3h^2}\,A_{44}\gamma_{0,x}\Big(\frac{5}{4}\gamma_{0,x} - w_{,xx}\Big) + \frac{25}{9h^4}\,A_{66}\gamma_{,x}^2 + 25\Big(\frac{1}{16}\,B_{11} - \frac{1}{2h^2}B_{22} + \frac{1}{h^4}\,B_{44}\Big)\gamma_0^2\Big]\mathrm{d}x, \end{aligned} \tag{8}$$

where L and A are, respectively, the total beam length and cross-sectional area; A_{11}, A_{12}, A_{22}, A_{34}, A_{44}, A_{66}, B_{11}, B_{22} and B_{44} are the beam rigidities, defined as

$$
\begin{aligned}
(A_{11},\, A_{12},\, A_{22},\, A_{34},\, A_{44},\, A_{66}) &= b\sum_{k=1}^{3}\int_{z_{k-1}}^{z_k} E_f^{(k)}(x,z)(1,z,z^2,z^3,z^4,z^6)\,\mathrm{d}z,\\
(B_{11},\, B_{22},\, B_{44}) &= b\sum_{k=1}^{3}\int_{z_{k-1}}^{z_k} G_f^{(k)}(x,z)(1,z,z^2,z^3,z^4,z^6)\,\mathrm{d}z,
\end{aligned}
\tag{9}
$$

with b is the beam width.

The kinetic energy $\mathcal{T}$ resulted from Eq. (5) is

$$
\begin{aligned}
\mathcal{T} = \frac{1}{2}\int_0^L \Big[& I_{11}(\dot{u}^2+\dot{w}^2) + 2I_{12}\dot{u}\left(\frac{5}{4}\dot{\gamma}_0 - \dot{w}_{,x}\right) + I_{22}\left(\frac{5}{4}\dot{\gamma}_0 - \dot{w}_{,x}\right)^2\\
& - \frac{10}{3h^2}I_{34}\dot{u}\dot{\gamma}_0 - \frac{10}{3h^2}I_{44}\dot{\gamma}_0\left(\frac{5}{4}\dot{\gamma}_0 - \dot{w}_{,x}\right) + \frac{25}{9h^4}I_{66}\dot{\gamma}_0{}^2\Big]\mathrm{d}x,
\end{aligned}
\tag{10}
$$

where I_{11}, I_{12}, I_{22}, I_{34}, I_{44}, and I_{66} are the mass moments, defined as

$$
(I_{11},\, I_{12},\, I_{22},\, I_{34},\, I_{44},\, I_{66}) = b\sum_{k=1}^{3}\int_{z_{k-1}}^{z_k} \rho_f^{(k)}(x,z)(1,z,z^2,z^3,z^4,z^6)\,\mathrm{d}z,
\tag{11}
$$

with $\rho_f^{(k)}$ is the effective mass density, defined by Eq. (3).

4. FINITE ELEMENT FORMULATION

The beam rigidities and mass moments, as seen from in Eqs. (9) and (11), depend on the co-ordinate x, thus a closed-form solution for differential equation of motion of such a beam is hardly derived. Instead of deriving the differential equation of motion, the equation of motion in the context of finite element analysis for free vibration analysis will be derived. Assuming the beam is divided into a number of elements with length l, Hamilton's principle for free vibration states that

$$
\delta\int_{t_1}^{t_2}\sum^{\mathrm{NE}}(U_e - \mathcal{T}_e)\,\mathrm{d}t = 0,
\tag{12}
$$

where the summation is taken over the total number of elements NE; U_e and $\mathcal{T}_e$ are, respectively, the strain and kinetic energies of an element. The expressions for U_e and $\mathcal{T}_e$ are the same as Eqs. (8) and (10), respectively, but with a integral span of $[0, l]$. The Hamilton's principle leads to discretized equation of motion in the form

$$
\mathbf{M}\ddot{\mathbf{D}} + \mathbf{K}\mathbf{D} = \mathbf{0},
\tag{13}
$$

where $\mathbf{M}$, $\mathbf{K}$, $\mathbf{D}$, and $\ddot{\mathbf{D}}$ are, respectively, the global mass matrix, stiffness matrix, and vectors of nodal displacements and accelerations. Assuming a harmonic form for the

vector of nodal displacements, Eq. (13) leads to an eigenvalue problem for determining the frequency ω as

$$\left(\mathbf{K} - \omega^2 \mathbf{M}\right) \bar{\mathbf{D}} = \mathbf{0}, \tag{14}$$

with ω is the circular frequency and $\bar{\mathbf{D}}$ is the vibration amplitude. Eq. (14) leads to an eigenvalue problem, and its solution can be obtained by the standard method [23].

A two-node beam element with four degrees of freedom per node as in Ref. [21] is adopted herewith. The vector of nodal displacements is of the form

$$\mathbf{d} = \{u_1 \quad w_1 \quad w_{x1} \quad \gamma_1 \quad u_2 \quad w_2 \quad w_{x2} \quad \gamma_2\}^T, \tag{15}$$

where u_i, w_i, w_{xi} and γ_i $(i = 1, 2)$ are, respectively, the values of u, w, $w_{,x}$ and γ_0 at the node i; a superscript 'T' in (15) and hereafter is used to denote the transpose of a vector or a matrix.

The axial displacement $u(x,t)$ and transverse shear rotation $\gamma_0(x,t)$ are linearly interpolated, while cubic Hermite polynomials are used for the transverse displacement $w(x,t)$. In this regard, and following same procedure as in [21] one can express the strain and kinetic energies of the element in the forms

$$U_e = \frac{1}{2}\sum^{\mathrm{NE}} \mathbf{d}^T \mathbf{k}_e \, \mathbf{d}\,, \quad \mathcal{T}_e = \frac{1}{2}\sum^{\mathrm{NE}} \dot{\mathbf{d}}^T \mathbf{m}_e \, \dot{\mathbf{d}}\,, \tag{16}$$

where $\mathbf{k}_e$ and $\mathbf{m}_e$ are, respectively, the element stiffness and mass matrices. The expressions for these matrices are as follows

$$\mathbf{k}_e = \mathbf{k}^{11}_{uu} + \mathbf{k}^{12}_{u\gamma} + \mathbf{k}^{22}_{\gamma w} + \mathbf{k}^{34}_{u\gamma} + \mathbf{k}^{44}_{\gamma\gamma} + \mathbf{k}^{66}_{\gamma\gamma} + \mathbf{k}_{ss}\,, \tag{17}$$

where

$$\begin{aligned}
\mathbf{k}^{11}_{uu} &= \int_0^l \mathbf{N}^T_{u,x} \, A_{11} \mathbf{N}_{u,x} \mathrm{d}x, \\
\mathbf{k}^{12}_{u\gamma} &= \int_0^l \left[\mathbf{N}^T_{u,x} \, A_{12} \left(\frac{5}{4}\mathbf{N}_{\gamma,x} - \mathbf{N}_{w,xx} \right) + \left(\frac{5}{4}\mathbf{N}_{\gamma,x} - \mathbf{N}_{w,xx} \right)^T A_{12} \mathbf{N}_{u,x} \right] \mathrm{d}x, \\
\mathbf{k}^{22}_{\gamma w} &= \int_0^l \left(\frac{5}{4}\mathbf{N}_{\gamma,x} - \mathbf{N}_{w,xx} \right)^T A_{22} \left(\frac{5}{4}\mathbf{N}_{\gamma,x} - \mathbf{N}_{w,xx} \right) \mathrm{d}x, \\
\mathbf{k}^{34}_{u\gamma} &= -\frac{5}{3h^2} \int_0^l \left[\mathbf{N}^T_{u,x} \, A_{34} \mathbf{N}_{\gamma,x} + \mathbf{N}^T_{\gamma,x} A_{34} \mathbf{N}_{u,x} \right] \mathrm{d}x, \\
\mathbf{k}^{44}_{\gamma\gamma} &= -\frac{5}{3h^2} \int_0^l \left[\mathbf{N}^T_{\gamma,x} \, A_{44} \left(\frac{5}{4}\mathbf{N}_{\gamma,x} - \mathbf{N}_{w,xx} \right) + \left(\frac{5}{4}\mathbf{N}_{\gamma,x} - \mathbf{N}_{w,xx} \right)^T A_{44} \mathbf{N}_{\gamma,x} \right] \mathrm{d}x\,, \\
\mathbf{k}^{66}_{\gamma\gamma} &= \frac{25}{9h^4} \int_0^l \mathbf{N}^T_{\gamma,x} \, A_{66} \mathbf{N}_{\gamma,x} \mathrm{d}x, \qquad \mathbf{k}_{ss} = 25 \int_0^l \mathbf{N}^T_{\gamma} \left(\frac{1}{16} B_{11} - \frac{1}{2h^2} B_{22} + \frac{1}{h^4} B_{44} \right) \mathbf{N}_{\gamma} \mathrm{d}x,
\end{aligned} \tag{18}$$

and

$$\mathbf{m}_e = \mathbf{m}_{uu}^{11} + \mathbf{m}_{ww}^{11} + \mathbf{m}_{u\gamma}^{12} + \mathbf{m}_{\gamma w}^{22} + \mathbf{m}_{u\gamma}^{34} + \mathbf{m}_{\gamma\gamma}^{44} + \mathbf{m}_{\gamma\gamma}^{66}, \tag{19}$$

where

$$\begin{aligned}
\mathbf{m}_{uu}^{11} &= \int_0^l \mathbf{N}_u^T I_{11} \mathbf{N}_u \mathrm{d}x, \quad \mathbf{m}_{ww}^{11} = \int_0^l \mathbf{N}_w^T I_{11} \mathbf{N}_w \mathrm{d}x, \quad \mathbf{m}_{\gamma\gamma}^{66} = \frac{25}{9h^4} \int_0^l \mathbf{N}_\gamma^T I_{66} \mathbf{N}_\gamma \mathrm{d}x, \\
\mathbf{m}_{u\gamma}^{12} &= \int_0^l \left[\mathbf{N}_u^T I_{12} \left(\frac{5}{4}\mathbf{N}_\gamma - \mathbf{N}_{w,x} \right) + \left(\frac{5}{4}\mathbf{N}_\gamma - \mathbf{N}_{w,x} \right)^T I_{12} \mathbf{N}_u \right] \mathrm{d}x, \\
\mathbf{m}_{\gamma w}^{22} &= \int_0^l \left(\frac{5}{4}\mathbf{N}_\gamma - \mathbf{N}_{w,x} \right)^T I_{22} \left(\frac{5}{4}\mathbf{N}_\gamma - \mathbf{N}_{w,x} \right) \mathrm{d}x, \\
\mathbf{m}_{u\gamma}^{34} &= -\frac{5}{3h^2} \int_0^l \left[\mathbf{N}_u^T I_{34} \mathbf{N}_\gamma + \mathbf{N}_\gamma^T I_{34} \mathbf{N}_u \right] \mathrm{d}x, \\
\mathbf{m}_{\gamma\gamma}^{44} &= -\frac{5}{3h^2} \int_0^l \left[\mathbf{N}_\gamma^T I_{44} \left(\frac{5}{4}\mathbf{N}_\gamma - \mathbf{N}_{w,x} \right) + \left(\frac{5}{4}\mathbf{N}_\gamma - \mathbf{N}_{w,x} \right)^T I_{44} \mathbf{N}_\gamma \right] \mathrm{d}x.
\end{aligned} \tag{20}$$

In Eqs. (18) and (20), $\mathbf{N}_u$, $\mathbf{N}_\gamma$ and $\mathbf{N}_w$ are, respectively, the matrices of the interpolation functions for u, γ_0 and w as stated in [21]. Gauss quadrature is used herein to evaluate the integrals in Eqs. (18) and (20).

5. NUMERICAL RESULTS

Aluminum (Al), zirconia (ZrO_2) and alumina (Al_2O_3) are respectively employed as M1, M2 and M3 for a softcore beam used in this section. The material properties of these constituent materials adopted from [9] are given in Tab. 1. Three types of boundary conditions, namely simply supported (SS), clamped at both ends (CC) and clamped at left end and free at the other (CF), are considered. The frequency parameter is defined as

$$\mu_i = \omega_i \frac{L^2}{h} \sqrt{\frac{\rho_{\mathrm{Al}}}{E_{\mathrm{Al}}}}, \tag{21}$$

where ω_i is the ith natural frequency. The layer thickness ratio, as in Ref. [9], is denoted by three numbers in brackets, e.g. (1-2-1) means that the thickness ratio of the bottom, core and top layers is 1:2:1.

The accuracy and convergence of the derived element are firstly verified. Since the beam model is proposed herein for the first time, and no data of its frequencies are available, the verification is carried for a special case of a unidirectional FGSW beam. Since Eq. (1) results in $V_2 = 0$ when $n_x = 0$, and in this case the 2D-FGSW beam becomes a unidirectional FGSW beam formed from M1 and M3 with material properties vary in the thickness direction only. Thus, the frequencies of the unidirectional FGSW beam can be obtained from the present formulation by simply setting n_x to zero. Table 2 lists the

Table 1. Material properties of constituent materials for the 2D-FGSW beam

Property	Aluminum	Alumina	Zirconia
Young's modulus (E, GPa)	70	380	150
Density (ρ, kg/m^3)	2702	3960	3000
Poison's ratio (ν)	0.3	0.3	0.3

fundamental frequencies of the unidirectional FGSW beam with $L/h = 20$, obtained in the present work, where the result of Ref. [9] is also given. Regardless of the aspect ratio, the material index and layer thickness ratio, a good agreement between the result of the present work with that of Ref. [9] is noted from Tab. 2.

Table 2. Comparison of frequency parameter μ_1 of SS beam with $n_x = 0$ and $L/h = 20$

n_z	Source	1-0-1	2-1-2	2-1-1	1-1-1	2-2-1	1-2-1	1-8-1
0	Ref. [9]	2.8371	2.8371	2.8371	2.8371	2.8371	2.8371	2.8371
	Present	2.8353	2.8353	2.8353	2.8353	2.8353	2.8353	2.8353
0.5	Ref. [9]	4.8579	4.7460	4.6050	4.6294	4.4611	4.4160	3.7255
	Present	4.8416	4.7311	4.6274	4.6156	4.4856	4.4040	3.7186
1	Ref. [9]	5.2990	5.2217	5.0541	5.1160	4.9121	4.8938	4.0648
	Present	5.2931	5.2147	5.0942	5.1086	4.9569	4.8863	4.0600
2	Ref. [9]	5.5239	5.5113	5.3390	5.4410	5.2242	5.2445	4.3542
	Present	5.5184	5.5043	5.3798	5.4330	5.2754	5.2358	4.3483
5	Ref. [9]	5.5645	5.6382	5.4834	5.6242	5.4166	5.4843	4.5991
	Present	5.5599	5.6320	5.5168	5.6166	5.4667	5.4752	4.5922
10	Ref. [9]	5.5302	5.6452	5.5073	5.6621	5.4667	5.5575	4.6960
	Present	5.5266	5.6392	5.5347	5.6545	5.5134	5.5483	4.6889

The convergence of the derived element is shown in Tab. 3, where the fundamental frequency parameters of the SS beam obtained by different number of the elements are given for various grading indexes and layer thickness ratios. As seen from the table, the unidirectional FGSW needs only 14 element to achieve the convergence, while the 2D-FGSW beam requires 24 elements. Thus, the longitudinal variation of the material properties considerably slows down the convergence of the element. Because of this convergence result, a mesh of 24 elements are used in all the computations reported below.

The fundamental frequency parameters of the 2D-FGSW beam with an aspect ratio $L/h = 20$ are given in Tabs. 4, 5 and 6 for the SS, CC and CF beams, respectively. As seen from the tables, the frequency parameter increases by increasing the index n_z, but it decreases by the increase of the n_x, irrespective of the layer thickness ratio and the boundary conditions. The dependence of the frequency parameter upon the material

Table 3. Convergence of the element in evaluating fundamental frequencies of SS beam $(L/h = 20)$

Beam	n_x	n_z	NE = 10	NE = 12	NE = 14	NE = 16	NE = 18	NE = 20	NE = 22	NE = 24
(2-1-2)	0	0.5	4.7312	4.7311	4.7311	4.7311	-	-	-	-
		1	5.2148	5.2147	5.2147	5.2147	-	-	-	-
		2	5.0045	5.0043	5.0043	5.0043	-	-	-	-
		5	5.6322	5.6320	5.6320	5.6320	-	-	-	
(2-2-1)	0	0.5	4.4859	4.4858	4.4857	4.4856	4.4856	-	-	-
		1	4.9573	4.9572	4.9571	4.9569	4.9569	-	-	
		2	5.2757	5.2756	5.2755	5.2754	5.2754	-	-	
		5	5.4672	5.4670	5.4668	5.4667	5.4667	-	-	-
(2-1-2)	2	0.5	3.9141	3.9143	3.9144	3.9145	3.9145	3.9146	3.9146	3.9146
		1	4.2544	4.2547	4.2549	4.2550	4.2551	4.2552	4.2552	4.2552
		2	4.4881	4.4885	4.4887	4.4889	4.4890	4.4891	4.4892	4.4892
		5	4.6236	4.6241	4.6244	4.6246	4.6247	4.6248	4.6249	4.6249
(2-2-1)	2	0.5	3.7513	3.7515	3.7516	3.7516	3.7516	3.7516	3.7516	3.7516
		1	4.0630	4.0631	4.0632	4.0633	4.0634	4.0634	4.0634	4.0634
		2	4.2947	4.2950	4.2951	4.2952	4.2953	4.2953	4.2953	4.2953
		5	4.4534	4.4536	4.4538	4.4539	4.4540	4.4541	4.4541	4.4541

Table 4. Fundamental frequency parameter of SS beam with $L/h = 20$ for various grading indexes and layer thickness ratios

n_x	n_z	1-0-1	2-1-2	2-1-1	1-1-1	2-2-1	1-2-1	1-8-1
0.3	0	2.8353	2.8353	2.8353	2.8353	2.8353	2.8353	2.8353
	0.3	4.3280	4.2081	4.1257	4.0994	3.9968	3.9191	3.4063
	0.5	4.7630	4.6296	4.5261	4.5028	4.3734	4.2842	3.6264
	1	5.2687	5.1460	5.0200	5.0138	4.8557	4.7664	3.9445
	2	5.5648	5.4872	5.3512	5.3752	5.2033	5.1337	4.2191
	5	5.6814	5.6752	5.5431	5.6063	5.4343	5.4017	4.4564
0.5	0	2.8353	2.8353	2.8353	2.8353	2.8353	2.8353	2.8353
	0.3	4.2269	4.1116	4.0341	4.0082	3.9119	3.8380	3.3598
	0.5	4.6429	4.5122	4.4140	4.3898	4.2674	4.1813	3.5639
	1	5.1347	5.0096	4.8887	4.8791	4.7276	4.6394	3.8605
	2	5.4313	5.3448	5.2129	5.2304	5.0639	4.9922	4.1182
	5	5.5586	5.5364	5.4067	5.4600	5.2917	5.2531	4.3422
1	0	2.8353	2.8353	2.8353	2.8353	2.8353	2.8353	2.8353
	0.3	3.9989	3.9001	3.8347	3.8120	3.7308	3.6678	3.2671
	0.5	4.3564	4.2429	4.1592	4.1375	4.0333	3.9590	3.4373
	1	4.7849	4.6738	4.5695	4.5595	4.4292	4.3516	3.6865
	2	5.0481	4.9682	4.8533	4.8662	4.7216	4.6572	3.9047
	5	5.1654	5.1396	5.0257	5.0692	4.9219	4.8853	4.0957
5	0	2.8353	2.8353	2.8353	2.8353	2.8353	2.8353	2.8353
	0.3	3.4642	3.4089	3.3725	3.3593	3.3144	3.2785	3.0592
	0.5	3.6728	3.6078	3.5602	3.5471	3.4881	3.4444	3.1514
	1	3.9284	3.8644	3.8034	3.7973	3.7216	3.6747	3.2900
	2	4.0863	4.0422	3.9737	3.9825	3.8972	3.8580	3.4144
	5	4.1537	4.1446	4.0761	4.1052	4.0175	3.9962	3.5254

Table 5. Fundamental frequency parameters of CC beam with $L/h = 20$ for various grading indexes and layer thickness ratios

n_x	n_z	1-0-1	2-1-2	2-1-1	1-1-1	2-2-1	1-2-1	1-8-1
0.3	0	6.3324	6.3324	6.3324	6.3324	6.3324	6.3324	6.3324
	0.3	9.4021	9.1394	8.9369	8.9100	8.6669	8.5386	7.5011
	0.5	10.3011	9.9988	9.7378	9.7254	9.4101	9.2716	7.9467
	1	11.3627	11.0623	10.7395	10.7630	10.3662	10.2360	8.5856
	2	12.0085	11.7856	11.4386	11.5119	11.0727	10.9743	9.1322
	5	12.2931	12.2126	11.8814	12.0150	11.5717	11.5272	9.6011
0.5	0	6.3324	6.3324	6.3324	6.3324	6.3324	6.3324	6.3324
	0.3	9.1858	8.9360	8.7487	8.7194	8.4944	8.3709	7.4062
	0.5	10.0391	9.7478	9.5047	9.4870	9.1935	9.0576	7.8185
	1	11.0620	10.7642	10.4606	10.4738	10.1012	9.9693	8.4127
	2	11.7007	11.4670	11.1374	11.1951	10.7793	10.6744	8.9242
	5	12.0018	11.8940	11.5759	11.6878	11.2643	11.2074	9.3655
1	0	6.3324	6.3324	6.3324	6.3324	6.3324	6.3324	6.3324
	0.3	8.8262	8.6054	8.4429	8.4141	8.2188	8.1072	7.2625
	0.5	9.5857	9.3262	9.1140	9.0944	8.8383	8.7139	7.6224
	1	10.5052	10.2363	9.9689	9.9761	9.6486	9.5260	8.1442
	2	11.0873	10.8714	10.5786	10.6253	10.2574	10.1587	8.5962
	5	11.3703	11.2617	10.9769	11.0713	10.6946	10.6389	8.9886
5	0	6.3324	6.3324	6.3324	6.3324	6.3324	6.3324	6.3324
	0.3	8.1139	7.9558	7.8414	7.8179	7.6802	7.5960	6.9879
	0.5	8.6739	8.4874	8.3365	8.3193	8.1371	8.0414	7.2465
	1	9.3576	9.1650	8.9719	8.9762	8.7406	8.6459	7.6260
	2	9.7902	9.6385	9.4247	9.4617	9.1948	9.1206	7.9590
	5	9.9962	9.9263	9.7165	9.7926	9.5178	9.4801	8.2507

Table 6. Fundamental frequency parameters of CF beam with $L/h = 20$ for various grading indexes and layer thickness ratios

n_x	n_z	1-0-1	2-1-2	2-1-1	1-1-1	2-2-1	1-2-1	1-8-1
0.3	0	1.0127	1.0127	1.0127	1.0127	1.0127	1.0127	1.0127
	0.3	1.4454	1.4106	1.3811	1.3788	1.3438	1.3260	1.1763
	0.5	1.5744	1.5357	1.4971	1.4985	1.4525	1.4340	1.2403
	1	1.7249	1.6899	1.6413	1.6513	1.5925	1.5781	1.3337
	2	1.8123	1.7916	1.7391	1.7596	1.6942	1.6884	1.4151
	5	1.8451	1.8466	1.7969	1.8281	1.7626	1.7689	1.4859
0.5	0	1.0127	1.0127	1.0127	1.0127	1.0127	1.0127	1.0127
	0.3	1.3809	1.3502	1.3254	1.3225	1.2930	1.2768	1.1493
	0.5	1.4943	1.4595	1.4267	1.4264	1.3874	1.3699	1.2035
	1	1.6293	1.5964	1.5546	1.5612	1.5107	1.4957	1.2831
	2	1.7103	1.6887	1.6429	1.6584	1.6016	1.5935	1.3531
	5	1.7436	1.7406	1.6965	1.7214	1.6638	1.6658	1.4145
1	0	1.0127	1.0127	1.0127	1.0127	1.0127	1.0127	1.0127
	0.3	1.2907	1.2667	1.2483	1.2452	1.2233	1.2100	1.1133
	0.5	1.3801	1.3524	1.3277	1.3263	1.2969	1.2820	1.1541
	1	1.4886	1.4616	1.4295	1.4332	1.3946	1.3809	1.2149
	2	1.5551	1.5366	1.5009	1.5115	1.4675	1.4589	1.2689
	5	1.5834	1.5796	1.5447	1.5631	1.5179	1.5174	1.3168
5	0	1.0127	1.0127	1.0127	1.0127	1.0127	1.0127	1.0127
	0.3	1.2051	1.1880	1.1754	1.1727	1.1576	1.1477	1.0801
	0.5	1.2707	1.2506	1.2333	1.2317	1.2110	1.1996	1.1085
	1	1.3515	1.3319	1.3089	1.3109	1.2833	1.2723	1.1514
	2	1.4014	1.3883	1.3622	1.3698	1.3380	1.3307	1.1904
	5	1.4221	1.4205	1.3947	1.4087	1.3757	1.3747	1.2253

grading index n_z can be explained by the change of the effective Young's modulus as shown by Eqs. (1) and (3). An increase of n_z leads to an increase of volume fraction of Al_2O_3 and ZrO_2. Since Young's modulus of Al is much lower than that of Al_2O_3 and ZrO_2, the effective modulus increases by increasing n_z and this results in an increase of the beam rigidities. The mass moments also increase by increasing the index n_z, but this increase is much lower than that of the rigidities. As a result, the frequencies increase by increasing n_z. A similar argument can be explained for the decrease of the frequencies by increasing n_x. The numerical result in Tabs. 4–6 reveals that the variation of the material properties in the length direction plays an important role in the frequencies of the 2D-FGSW beams, and a desired frequency can be obtained by approximate choice of the material grading indexes.

In addition to the material grading indexes, Tabs. 4–6 also show an important role of the layer thickness ratio on the frequency of the sandwich beam. A larger core thickness the beam has a smaller frequency parameter is, regardless of the material index and the boundary conditions. However, change of the frequency parameter by the change of the layer thickness ratio is different between the symmetrical and asymmetrical beams.

The variation of the first four frequency parameters μ_i $(i = 1, \ldots, 4)$ with the material grading indexes is displayed in Figs. 3–5 for the SS, CC and CF beams, respectively. The figures are obtained for the (2-1-2) beams with an aspect ratio $L/h = 20$. The dependence of the higher frequency parameters upon the grading indexes is similar to that of the fundamental frequency parameter. All the frequency parameters increase by increasing the index n_z, and they decrease by the increase of the index n_x, regardless of the boundary conditions.

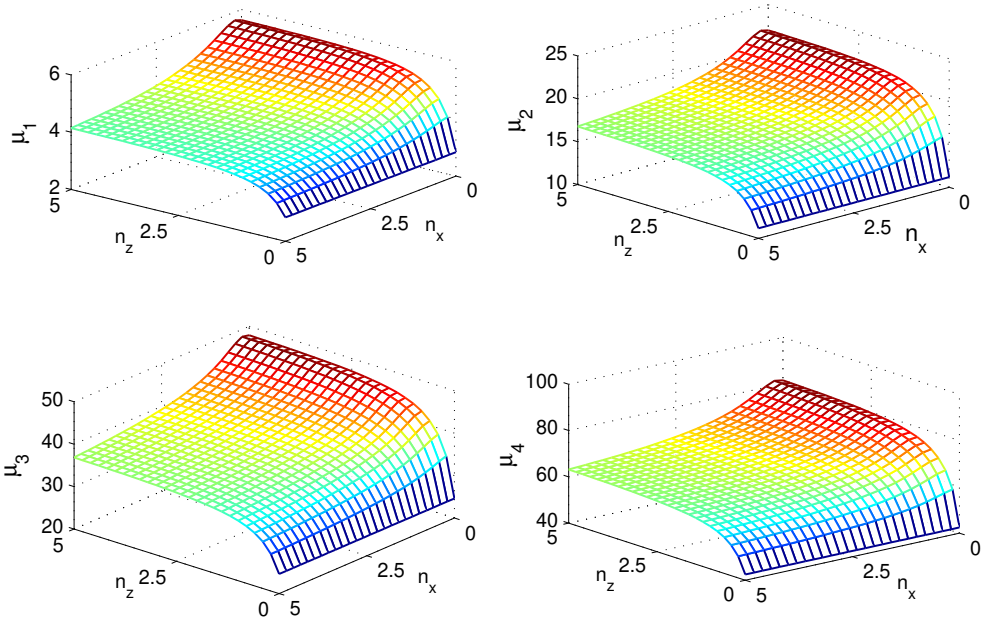

Fig. 3. Variation of the first four frequency parameters of (2-1-2) SS beam with grading indexes

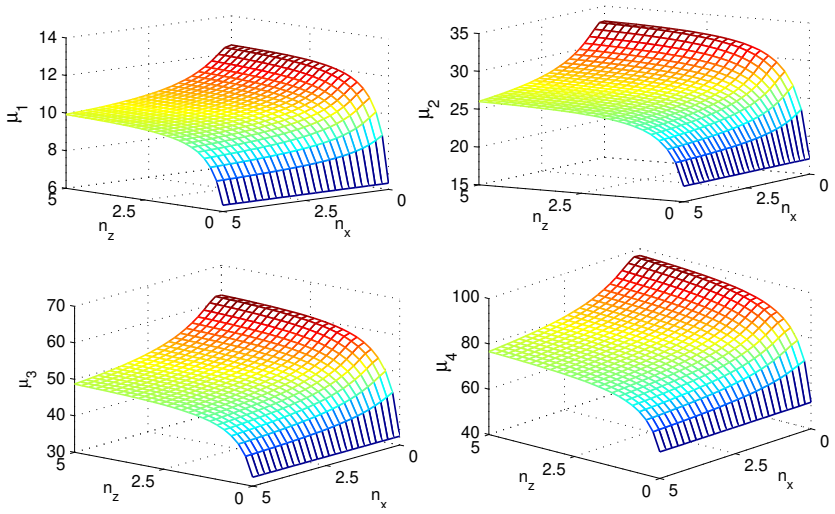

Fig. 4. Variation of the first four frequency parameters of (2-1-2) CC beam with grading indexes

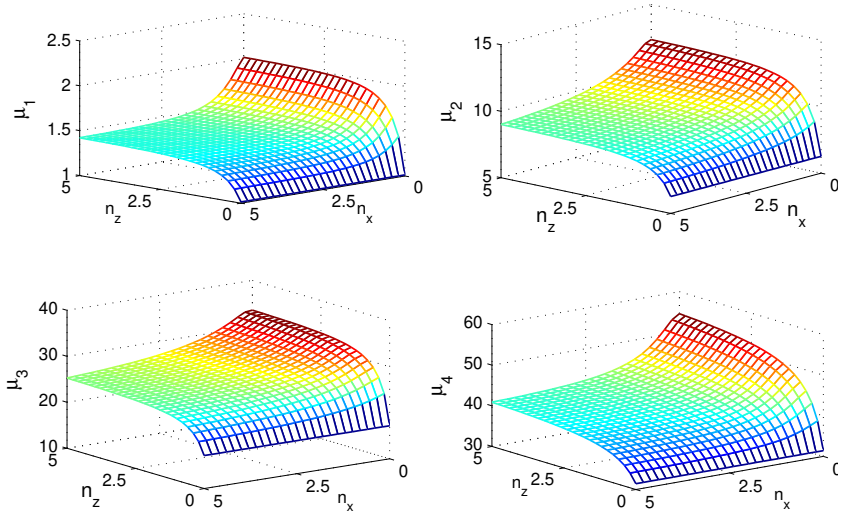

Fig. 5. Variation of the first four frequency parameters of (2-1-2) CF beam with grading indexes

To examine the effect of the aspect ratio on the frequencies of the beam, Tab. 7 lists the fundamental frequency parameter of the SS beam with an aspect ratio $L/h = 5$. By comparing Tab. 7 with Tab. 4 one can see that the frequency parameter of the beam with $L/h = 5$ is lower than that of the beam with $L/h = 20$. The effect of the aspect ratio on the frequency parameter can also be seen from Fig. 6, where the aspect ratio versus the frequency parameter μ_1 is shown for the SS and CF beams with various values of the layer thickness ratio. Regardless of the layer thickness ratio and the boundary conditions, the frequency parameter increases by the increase of the aspect ratio. The layer thickness

ratio can change the frequency amplitude, but it hardly change the dependence of the frequency on the aspect ratio. The numerical result in Tab. 7 and Fig. 6 shows the ability of the formulated element in modelling the shear deformation effect of the 2D-FGSW beams.

Table 7. Fundamental frequency parameters of SS beam with $L/h = 5$

n_x	n_z	1-0-1	2-1-2	2-1-1	1-1-1	2-2-1	1-2-1	1-8-1
0.3	0	2.6540	2.6540	2.6540	2.6540	2.6540	2.6540	2.6540
	0.3	3.9317	3.8075	3.7456	3.7068	3.6266	3.5530	3.1377
	0.5	4.3056	4.1543	4.0789	4.0297	3.9311	3.8396	3.3171
	1	4.7611	4.5904	4.5009	4.4416	4.3231	4.2107	3.5690
	2	5.0623	4.9055	4.8084	4.7507	4.6207	4.4964	3.7789
	5	5.2282	5.1197	5.0214	4.9810	4.8464	4.7219	3.9550
0.5	0	2.6540	2.6540	2.6540	2.6540	2.6540	2.6540	2.6540
	0.3	3.8472	3.7298	3.6710	3.6346	3.5587	3.4893	3.0996
	0.5	4.2045	4.0604	3.9880	3.9421	3.8478	3.7613	3.2670
	1	4.6447	4.4799	4.3929	4.3377	4.2232	4.1172	3.5040
	2	4.9413	4.7859	4.6907	4.6367	4.5100	4.3932	3.7035
	5	5.1114	4.9970	4.9000	4.8605	4.7285	4.6113	3.8723
1	0	2.6540	2.6540	2.6540	2.6540	2.6540	2.6540	2.6540
	0.3	3.6573	3.5579	3.5073	3.4769	3.4119	3.3528	3.0224
	0.5	3.9658	3.8437	3.7805	3.7428	3.6610	3.5874	3.1634
	1	4.3486	4.2090	4.1321	4.0882	3.9876	3.8984	3.3656
	2	4.6077	4.4757	4.3911	4.3495	4.2378	4.1414	3.5382
	5	4.7577	4.6589	4.5725	4.5436	4.4270	4.3324	3.6858
5	0	2.6540	2.6540	2.6540	2.6540	2.6540	2.6540	2.6540
	0.3	3.2090	3.1516	3.1222	3.1045	3.0671	3.0325	2.8464
	0.5	3.3951	3.3237	3.2858	3.2640	3.2154	3.1714	2.9244
	1	3.6307	3.5497	3.5018	3.4780	3.4161	3.3629	3.0403
	2	3.7897	3.7155	3.6618	3.6419	3.5719	3.5163	3.1429
	5	3.8779	3.8264	3.7714	3.7616	3.6883	3.6370	3.2332

In Fig. 7, the first three vibration modes for the transverse displacement w and transverse shear rotation γ_0 of the (1-1-1) SS beam are shown for two pairs of the grading indexes, $(n_x, n_z) = (0, 2)$ and $(n_x, n_z) = (2, 2)$. When $n_x = 0$, the beam becomes a unidirectional FGSW beam formed from M1 and M3, and thus Fig. 7 illustrates the vibration modes of the unidirectional FGSW beam. The effect of the variation of the material properties in the longitudinal direction can be seen by comparing Fig. 7(a) and Fig. 7(b). The symmetrical shape with respect to the mid-line of the first mode of the transverse displacement as seen in Fig. 7(a) is no longer seen for the 2D-FGSW beam in Fig. 7(a). The difference in the vibration modes of the transverse shear rotation of the unidirectional FGSW beam with that of the 2D-FGSW beam can also be seen from Fig. 7.

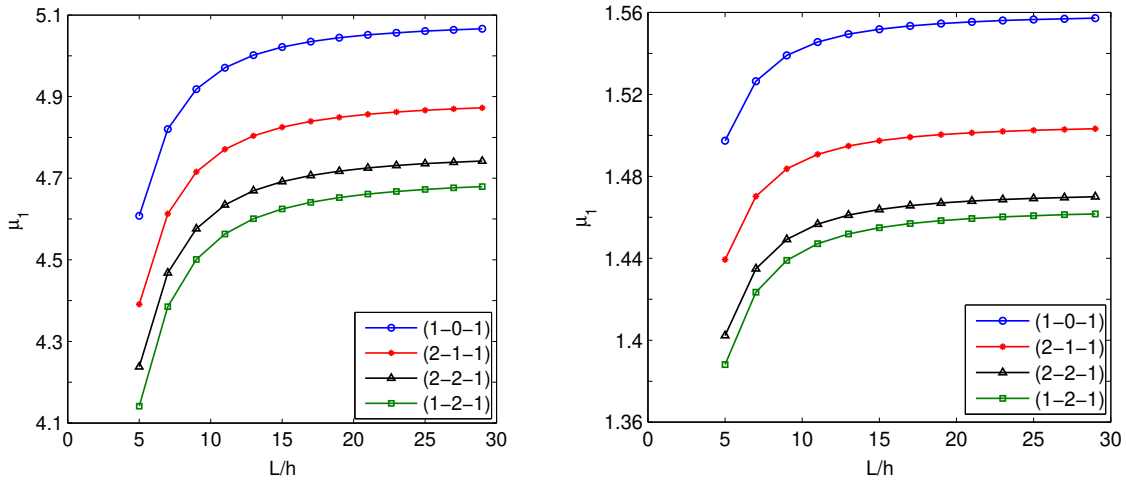

(a) SS beam (b) CF beam

Fig. 6. Aspect ratio L/h versus frequency parameter μ_1 of the 2D-FGSW beam with $n_x = n_z = 2$

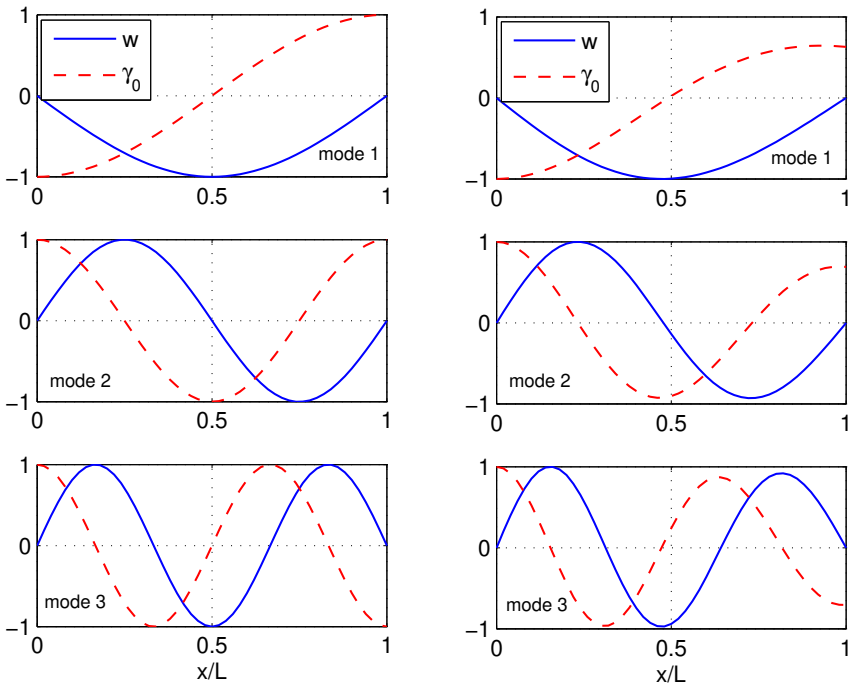

(a) $(n_x, n_z) = (0, 2)$ (b) $(n_x, n_z) = (2, 2)$

Fig. 7. The first three vibration modes for w and γ_0 of (1-1-1) SS beam

6. CONCLUSIONS

A 2D-FGSW beam model formed from three constituent materials has been proposed and its free vibration was studied. The beam consists of three layers, a homogeneous core and two FGM skin layers with material properties varying in both the thickness and longitudinal directions by the power gradation laws. Based on a third-order shear deformation theory, a beam element was formulated and employed in computing the vibration characteristics. It has been shown that the formulated element is accurate, and it is capable to model the effect of shear deformation on the frequencies of the beam. The obtained numerical result reveals that the variation of the material properties in the longitudinal direction plays an important role in the frequencies and vibration modes of the beam. A parametric study has been carried out to highlight the effects of the material distribution and the layer thickness ratio on the frequencies of the beam. The influence of the aspect ratio on the vibration behaviour of the beam has also been examined and discussed. It is necessary to note that the present beam model is new, and only free vibration of the beam is considered so far. Investigations on forced vibration and nonlinear bending of the beam should be carried out for understanding the mechanical behavior of the beam in more detail.

ACKNOWLEDGEMENT

This work was supported by Vietnam National Foundation for Science and Technology Development (NAFOSTED) under grant number 107.02-2018.23.

REFERENCES

[1] Y. Fukui. Fundamental investigation of functionally graded materials manufacturing system using centrifugal force. *JSME International Journal, Series 3*, **34**, (1991), pp. 144–148.

[2] M. Koizumi. FGM activities in Japan. *Composites Part B: Engineering*, **28**, (1-2), (1997), pp. 1–4. https://doi.org/10.1016/s1359-8368(96)00016-9.

[3] A. Chakraborty, S. Gopalakrishnan, and J. N. Reddy. A new beam finite element for the analysis of functionally graded materials. *International Journal of Mechanical Sciences*, **45**, (3), (2003), pp. 519–539. https://doi.org/10.1016/s0020-7403(03)00058-4.

[4] N. A. Apetre, B. V. Sankar, and D. R. Ambur. Analytical modeling of sandwich beams with functionally graded core. *Journal of Sandwich Structures & Materials*, **10**, (1), (2008), pp. 53–74. https://doi.org/10.1177/1099636207081111.

[5] S. C. Pradhan and T. Murmu. Thermo-mechanical vibration of FGM sandwich beam under variable elastic foundations using differential quadrature method. *Journal of Sound and Vibration*, **321**, (1-2), (2009), pp. 342–362. https://doi.org/10.1016/j.jsv.2008.09.018.

[6] O. Rahmani, S. M. R. Khalili, K. Malekzadeh, and H. Hadavinia. Free vibration analysis of sandwich structures with a flexible functionally graded syntactic core. *Composite Structures*, **91**, (2), (2009), pp. 229–235. https://doi.org/10.1016/j.compstruct.2009.05.007.

[7] M. C. Amirani, S. M. R. Khalili, and N. Nemati. Free vibration analysis of sandwich beam with FG core using the element free Galerkin method. *Composite Structures*, **90**, (3), (2009), pp. 373–379. https://doi.org/10.1016/j.compstruct.2009.03.023.

[8] A. M. Zenkour, M. N. M. Allam, and M. Sobhy. Bending analysis of FG viscoelastic sandwich beams with elastic cores resting on Pasternak's elastic foundations. *Acta Mechanica*, **212**, (3-4), (2010), pp. 233–252. https://doi.org/10.1007/s00707-009-0252-6.

[9] T. P. Vo, H.-T. Thai, T.-K. Nguyen, A. Maheri, and J. Lee. Finite element model for vibration and buckling of functionally graded sandwich beams based on a refined shear deformation theory. *Engineering Structures*, **64**, (2014), pp. 12–22. https://doi.org/10.1016/j.engstruct.2014.01.029.

[10] T. P. Vo, H.-T. Thai, T.-K. Nguyen, F. Inam, and J. Lee. A quasi-3D theory for vibration and buckling of functionally graded sandwich beams. *Composite Structures*, **119**, (2015), pp. 1–12. https://doi.org/10.1016/j.compstruct.2014.08.006.

[11] R. Bennai, H. A. Atmane, and A. Tounsi. A new higher-order shear and normal deformation theory for functionally graded sandwich beams. *Steel and Composite Structures*, **19**, (3), (2015), pp. 521–546. https://doi.org/10.12989/scs.2015.19.3.521.

[12] Z. Su, G. Jin, Y. Wang, and X. Ye. A general Fourier formulation for vibration analysis of functionally graded sandwich beams with arbitrary boundary condition and resting on elastic foundations. *Acta Mechanica*, **227**, (5), (2016), pp. 1493–1514. https://doi.org/10.1007/s00707-016-1575-8.

[13] M. Şimşek and M. Al-Shujairi. Static, free and forced vibration of functionally graded (FG) sandwich beams excited by two successive moving harmonic loads. *Composites Part B: Engineering*, **108**, (2017), pp. 18–34. https://doi.org/10.1016/j.compositesb.2016.09.098.

[14] T. Vo-Duy, V. Ho-Huu, and T. Nguyen-Thoi. Free vibration analysis of laminated FG-CNT reinforced composite beams using finite element method. *Frontiers of Structural and Civil Engineering*, **13**, (2), (2019), pp. 324–336.

[15] M. Nemat-Alla and N. Noda. Edge crack problem in a semi-infinite FGM plate with a bi-directional coefficient of thermal expansion under two-dimensional thermal loading. *Acta Mechanica*, **144**, (3-4), (2000), pp. 211–229. https://doi.org/10.1007/bf01170176.

[16] C. F. Lü, W. Q. Chen, R. Q. Xu, and C. W. Lim. Semi-analytical elasticity solutions for bi-directional functionally graded beams. *International Journal of Solids and Structures*, **45**, (1), (2008), pp. 258–275. https://doi.org/10.1016/j.ijsolstr.2007.07.018.

[17] M. Şimşek. Bi-directional functionally graded materials (BDFGMs) for free and forced vibration of Timoshenko beams with various boundary conditions. *Composite Structures*, **133**, (2015), pp. 968–978. https://doi.org/10.1016/j.compstruct.2015.08.021.

[18] Z.-H. Wang, X.-H. Wang, G.-D. Xu, S. Cheng, and T. Zeng. Free vibration of two-directional functionally graded beams. *Composite Structures*, **135**, (2016), pp. 191–198. https://doi.org/10.1016/j.compstruct.2015.09.013.

[19] A. Karamanlı. Bending behaviour of two directional functionally graded sandwich beams by using a quasi-3D shear deformation theory. *Composite Structures*, **174**, (2017), pp. 70–86. https://doi.org/10.1016/j.compstruct.2017.04.046.

[20] D. K. Nguyen, Q. H. Nguyen, T. T. Tran, and V. T. Bui. Vibration of bi-dimensional functionally graded Timoshenko beams excited by a moving load. *Acta Mechanica*, **228**, (1), (2017), pp. 141–155. https://doi.org/10.1007/s00707-016-1705-3.

[21] T. T. Tran and D. K. Nguyen. Free vibration analysis of 2-D FGM beams in thermal environment based on a new third-order shear deformation theory. *Vietnam Journal of Mechanics*, **40**, (2), (2018), pp. 121–140. https://doi.org/10.15625/0866-7136/10503.

[22] G. Shi. A new simple third-order shear deformation theory of plates. *International Journal of Solids and Structures*, **44**, (13), (2007), pp. 4399–4417. https://doi.org/10.1016/j.ijsolstr.2006.11.031.

[23] M. Géradin and D. J. Rixen. *Mechanical vibrations: theory and application to structural dynamics*. John Wiley & Sons, 2nd edition, (1997).